arXiv:cond-mat/9704057v1 [cond-mat.str-el] 7 Apr 1997

A DMRG Study of Low-Energy Excitations and Low-Temperature Properties of Alternating Spin Systems

Swapan K. Pati[1], **S. Ramasesha**[1,3] **and Diptiman Sen**[2,3]

[1] *Solid State and Structural Chemistry Unit*

[2] *Centre for Theoretical Studies*

Indian Institute of Science, Bangalore 560012, India

[3] *Jawaharlal Nehru Centre for Advanced Scientific Research*

Jakkur Campus, Bangalore 560064, India

Abstract

We use the density matrix renormalization group (DMRG) method to study the ground and low-lying excited states of three kinds of uniform and dimerized alternating spin chains. The DMRG procedure is also employed to obtain low-temperature thermodynamic properties of these systems. We consider a $2N$ site system with spins s_1 and s_2 alternating from site to site and interacting via a Heisenberg antiferromagnetic exchange. The three systems studied correspond to (s_1, s_2) being equal to $(1, \frac{1}{2})$, $(\frac{3}{2}, \frac{1}{2})$ and $(\frac{3}{2}, 1)$; all of them have very similar properties. The ground state is found to be ferrimagnetic with total spin $s_G = N(s_1 - s_2)$. We find that there is a gapless excitation to a state with spin $s_G - 1$, and a gapped excitation to a state with spin $s_G + 1$. Surprisingly, the correlation length in the ground state is found to be very small for this gapless system. The DMRG analysis shows that the chain is susceptible to a conditional spin-Peierls instability. Furthermore, our studies of the magnetization, magnetic susceptibility χ and specific heat show strong magnetic-field dependences. The product χT shows a minimum as a function of temperature T at low magnetic fields; the minimum vanishes at high magnetic fields. This low-field behavior is in agreement with earlier experimental observations. The specific heat shows a maximum as a function of temperature, and the height of the maximum increases sharply at high magnetic fields. Although all the three systems show qualitatively similar behavior, there are some notable quantitative differences between the systems in which the site spin difference, $|s_1 - s_2|$, is large and small respectively.

PACS number: 75.50.Gg

1 Introduction

There have been a number of experimental efforts over the last several years to synthesize molecular systems showing spontaneous magnetization [1, 2, 3]. These studies have led to the recent realization of systems such as $NPNN$ (*para*-nitrophenyl nitronyl nitroxide) and $C_{60} - TDAE$ (Tetrakis Dimethyl Amino Ethylene) which show ferromagnetic to paramagnetic transition at low-temperatures. There also exist theoretical models [4, 5] that predict ferrimagnetism in organic polymer systems, but a truly extended organic ferrimagnet has not been synthesized although an oligomer with a ground state spin of $S = 9$ is now known. On the inorganic front, pursuit of molecular magnetism has been vigorous, and there has been success in the synthesis of molecular systems showing spontaneous magnetization at low-temperatures[6, 7]. These are quasi-one-dimensional bimetallic molecular magnets in which each unit cell contains two spins with different spin values [7]. These systems contain two transition metal ions per unit cell, with the general formula $ACu(pbaOH)(H_2O)_3.2H_2O$, where $pbaOH$ is 2-hydroxo-1,3-propylenebis(oxamato) and A=Mn, Fe, Co, Ni, and they belong to the alternating or mixed spin chain family [8]. These alternating spin compounds have been seen to exhibit ferrimagnetic behavior. It has been possible to vary the spin at each site from low values where quantum effects dominate to large values which are almost classical.

There have been a number of theoretical investigations for quantum ferrimagnetic systems in recent years [9, 10]. However, these models consider complicated multispin interactions, while very little is known about the simple Heisenberg model with purely quadratic interactions. There have been some analytic studies of alternating spin-1/spin-$\frac{1}{2}$ system [11] and a detailed spin-wave analysis followed by a DMRG study [12] corresponding to the $Cu - Ni$ bimetallic chain with the simple Heisenberg model. These studies confirm that these ferrimagnetic systems can be accurately described by a pure Heisenberg spin model.

Theoretical studies of alternating spin systems have so far been concerned only about the spin-1/spin-$\frac{1}{2}$ bimetallic chains; further, the thermodynamic properties have not been explored in detail. The thermodynamic behavior of these alternating spin compounds is very interesting [8, 13]. In very low magnetic fields, these systems show one-dimensional ferrimagnetic behavior. The χT vs. T (where χ is the magnetic susceptibility and T the temperature) plots show a rounded minimum. As the temperature is increased, χT decreases sharply, goes through a minimum before increasing gradually. The temperature at which this minimum occurs differs from system to system and depends on the site spins of the chain. The variation of the field induced magnetization with temperature is also interesting as the ground state is a magnetic state. At low magnetic fields, the magnetization decreases with increasing temperature at low temperatures. However, at moderate magnetic fields, with increase in temperature, the magnetization slowly increases, shows a broad peak and then decreases. Such a behavior has been studied theoretically by us

for the spin-1/spin-$\frac{1}{2}$ system [12].

These interesting observations have motivated us to study of ferrimagentic systems with arbitrary spins s_1 and s_2 alternating from site to site. It would be quite interesting to know the thermodynamic properties of these systems with varying s_1 and s_2. In the previous paper, we predicted some interesting features of the thermodynamic properties of the spin-1/spin-$\frac{1}{2}$ system at high magnetic fields. We focus on the high field behavior of the general ferrimagnetic chains to find whether the observed properties are generic to these systems or are dependent on specific s_1 and s_2 values.

In this paper, we study the low-lying excited states and low-temperature properties of the spin-$\frac{3}{2}$/spin-1 and spin-$\frac{3}{2}$/spin-$\frac{1}{2}$ chains and rings and compare them with with those of the corresponding spin-1/spin-$\frac{1}{2}$ systems. We have employed the density matrix renormalization group (DMRG) method which has proved to be the best numerical tool for low-dimensional spin systems in recent years [14]. The ground state energy per site, the spin excitation gap and the two-spin correlation functions obtained from this method have been found to be accurate to several decimal places [15, 16, 17] when compared with Bethe-ansatz results (where possible) and exact diagonalization results of small systems. In the DMRG method, spin parity symmetry can be used to characterize the spin states along with the S^z_{tot} as the good quantum numbers. The DMRG calculations have been carried out on chains and rings with alternate spin-s_1/spin-s_2 sites, with s_1 fixed at $\frac{3}{2}$ and s_2 being 1 or $\frac{1}{2}$. Studies of the ground state and low-lying excited states are reported in detail and compared with those of $s_1 = 1$ and $s_2 = \frac{1}{2}$ system. Furthermore, by resorting to a full diagonalization of the DMRG Hamiltonian matrix in different S_z sectors, we have also obtained the low-temperature thermodynamic properties of these systems. The theromodynamic properties we discuss will include low and high field magnetization, magnetic susceptibilty and specific heat, all at low temperatures.

The paper is organized as follows. In section 2, we present properties of the ground and low-lying excited states and compare them with the results of spin wave theory. In section 3, we discuss the low-temperature thermodynamic properties of the systems. We summarize our results in the last section.

2 Ground State and Excitation Spectrum

We start our discussion with the Hamiltonian for a chain with spins s_1 and s_2 on alternating sites (with $s_1 > s_2$, without loss of generality).

$$H \;=\; J \sum_n \; [\; (1+\delta)\; \vec{S}_{1,n} \cdot \vec{S}_{2,n} \;+\; (1-\delta)\; \vec{S}_{2,n} \cdot \vec{S}_{1,n+1} \;] \;, \tag{1}$$

where the total number of sites is $2N$ and the sum is over the total number of unit cells N. $\vec{S}_{i,n}$ corresponds to the spin operator for the site spin s_i in the n-th unit cell. The

exchange integral J is taken to be positive for all our calculations; δ is the dimerization parameter and it lies in the range $[0, 1]$.

2.1 Summary of results from spin-wave theory

Before describing our numerical results, we briefly summarize the results of a spin wave analysis for the purposes of comparison [12]. We will first state the results with $\delta = 0$. According to spin wave theory, the ground state has total spin $s_G = N(s_1 - s_2)$. Let us define a function

$$\omega(k) \;=\; J\,\sqrt{(s_1 - s_2)^2 + 4 s_1 s_2 \sin^2(k/2)}\;, \tag{2}$$

where k denotes the wave number. Then the ground state energy per site is given by

$$\epsilon_0 \;=\; \frac{E_0}{2N} \;=\; -\;Js_1 s_2 \;+\; \frac{1}{2}\int_0^\pi \frac{dk}{\pi}\;[\;-\;J(s_1 + s_2)\;+\;\omega(k)\;]\;. \tag{3}$$

The lowest branch of excitations is to states with spin $s = s_G - 1$, with the dispersion

$$\omega_1(k) \;=\; J\;(-s_1 + s_2)\;+\;\omega(k)\;; \tag{4}$$

the gap vanishes at $k = 0$. There is a gapped branch of excitations to states with spin $s = s_G + 1$, with the dispersion

$$\omega_2(k) \;=\; J\;(s_1 - s_2)\;+\;\omega(k)\;; \tag{5}$$

the minimum gap occurs at $k = 0$ and is given by $\Delta = 2J(s_1 - s_2)$. In the ground state with $S_z = s_G$, the sublattice magnetizations are given by the expectation values

$$\begin{aligned} < S^z_{1,n} > \;&=\; (\;s_1 + \frac{1}{2}\;) \;-\; \frac{1}{2}\int_0^\pi \frac{dk}{\pi}\;\frac{J(s_1 + s_2)}{\omega}(k)\;, \\ < S^z_{2,n} > \;&=\; s_1 \;-\; s_2 \;-\; < S^z_{1,n} >\;. \end{aligned} \tag{6}$$

The various two-spin correlation functions decay exponentially with distance; the inverse correlation length is given by $\xi^{-1} = \ln(s_1/s_2)$. The results with dimerization ($\delta > 0$) are very similar. In fact, within spin wave theory, the minimum gap Δ to states with spin $s = s_G + 1$ is independent of δ.

2.2 Results from DMRG studies

We have studied the system defined by equation (1) both with and without dimerization, $\delta \neq 0$ and $\delta = 0$ respectively. We study alternating spin-$\frac{3}{2}$/spin-1 (hereafter designated as $(\frac{3}{2}, 1)$) and spin-$\frac{3}{2}$/spin-$\frac{1}{2}$ (to be called $(\frac{3}{2}, \frac{1}{2})$) chains with open boundary condition for the Hamiltonian (1) by employing the DMRG method. We compute the ground

state properties for both the systems by studying chains of upto 80 to 100 sites. The number of dominant density matrix eigenstates, m, that we have retained at each DMRG iteration also varies between 80 to 100 for both the systems. With the increase of the Fock space dimensionality of the site spins, we increase m to obtain more accurate results. The DMRG procedure follows the usual steps for chains discussed in earlier papers [14, 16, 17], except that the alternating chains studied here are not symmetric between the left and right halves; hence the density matrices for these two halves have to be constructed at every iteration of the calculations. We have verified the convergence of our results by varying the values of m and the system size. The ground states of both the system lie in the $S_z = N(s_1 - s_2)$ sector, as verified from extensive checks carried out by obtaining the low-energy eigenstates in different S_z sectors of a 20-site chain. A state corresponding to the lowest energy in $S_z = N(s_1 - s_2)$ is found in all subspaces with $|S_z| \leq N(s_1 - s_2)$, and is absent in subspaces with $|S_z| > N(s_1 - s_2)$. This shows that the spin in the ground state is $s_G = N(s_1 - s_2)$.

In a previous paper, we studied the alternating spin chain made up of spin-1 and spin-$\frac{1}{2}$ (hereafter refered as $(1, \frac{1}{2})$) at alternate sites [12]. We compare here the results for all the three systems, nemely, $(\frac{3}{2}, 1)$, $(\frac{3}{2}, 1/2)$ and $(1, \frac{1}{2})$ spin systems. In figure 1, we show the extrapolation of the energy per site as a function of inverse system size for all three systems. The ground state energy per site ϵ_0 extrapolates to $-1.93096J$ for the $(\frac{3}{2}, 1)$ system, to $-0.98362J$ for $(\frac{3}{2}, \frac{1}{2})$, and to $-0.72704J$ for $(1, \frac{1}{2})$. The spin wave analysis gives the values $-1.914J$ for $(\frac{3}{2}, 1)$, $-0.979J$ for $(\frac{3}{2}, \frac{1}{2})$ and $-0.718J$ for $(1, \frac{1}{2})$ which are all higher than the DMRG values. It is interesting to note that, in the alternating spin cases, the energy per site lies in between the values for the pure spin-s_1 uniform chain and the pure spin-s_2 uniform chain.

In figure 2, we show the expectation value of site spin operator $S^z_{i,n}$ (spin density) at all the sites for the $(\frac{3}{2}, 1)$, $(\frac{3}{2}, \frac{1}{2})$ and $(1, \frac{1}{2})$ chains. The spin densities are uniform on each of the sublattices in the chain for all the three systems. For the $(\frac{3}{2}, 1)$ chain, the spin density at a spin-$\frac{3}{2}$ is 1.14427 (the classical value is $\frac{3}{2}$), while, at a spin-1 site it is -0.64427 (classical value 1). For the $(\frac{3}{2}, \frac{1}{2})$ case, the spin density at a spin-$\frac{3}{2}$ site is 1.35742 and at a spin-$\frac{1}{2}$ site it is -0.35742. For the $(1, \frac{1}{2})$ case, the value at a spin-1 site is 0.79248 and at a spin-$\frac{1}{2}$ site it is -0.29248. These can be compared with the spin wave values of 1.040 and -0.540; 1.314 and -0.314; and 0.695 and -0.195 for the spin-s_1 and spin-s_2 sites of the $(\frac{3}{2}, 1)$; $(\frac{3}{2}, \frac{1}{2})$; and $(1, \frac{1}{2})$ systems respectively. We note that the spin wave analysis overestimates the quantum fluctuations in case of systems with small site spin values. We also notice that there is a greater quantum fluctuation when the difference in site spin $|s_1 - s_2|$ is larger. This is also seen in spin-wave theory. The spin density distribution in an alternating (s_1, s_2) chain behaves more like that in a ferromagnetic chain rather than like an antiferromagnet, with the net spin of each unit cell perfectly aligned (but with small quantum fluctuations on the individual sublattices). In a ferromagnetic ground state, the spin density at each site has the classical value appropriate to the site spin, whereas for an

antiferromagnet, this averages out to zero at each site as the ground state is nonmagnetic. From this viewpoint, the ferrimagnet is similar to a ferromagnet and is quite unlike an antiferromagnet. The spin wave analysis also yields the same physical picture.

Because of the alternation of spin-s_1 and spin-s_2 sites along the chain, one has to distinguish between three different types of pair correlations, namely, $< S^z_{1,0} S^z_{1,n} >$, $< S^z_{2,0} S^z_{2,n} >$ and $< S^z_{1,0} S^z_{2,n} >$. We calculate all the three correlation functions with the mean values subtracted out, since the mean values are nonzero in all these three systems unlike in pure antiferromagnetic spin chains. In the DMRG procedure, we have computed these correlation functions from the sites inserted at the last iteration, to minimize numerical errors. In figure 3, we plot the two-spin correlation functions in the ground state as a function of the distance between the spins for an open chain of 100 sites for all three cases. All three correlation functions decay rapidly with distance for each of the three systems. From the figure it is clear that, except for the $< S^z_{1,0} S^z_{2,n} >$ correlation, all other correlations are almost zero even for the shortest possible distances. The $< S^z_{1,0} S^z_{2,n} >$ correlation has an appreciable value [-0.2 for $(\frac{3}{2}, 1)$, -0.07 for $(\frac{3}{2}, \frac{1}{2})$ and -0.094 for $(1, \frac{1}{2})$] only for the nearest neighbors. This rapid decay of the correlation functions makes it difficult to find the exact correlation length ξ for a lattice model, although it is clear that ξ is very small (less than one unit cell) for the $(\frac{3}{2}, \frac{1}{2})$ and $(1, \frac{1}{2})$ cases, and a little greater ($1 < \xi < 2$) for the $(\frac{3}{2}, 1)$ system. Spin wave theory gives $\xi = 2.47$ for $(\frac{3}{2}, 1)$, $\xi = 0.91$ for $(\frac{3}{2}, \frac{1}{2})$, and $\xi = 1.44$ for $(1, \frac{1}{2})$ cases.

The lowest spin excitation of all the three chains is to a state with $s = s_G - 1$. To study this state, we target the 2nd state in the $S_z = s_G - 1$ sector of the chain. To confirm that this state is a $s = s_G - 1$ state, we have computed the 2-nd state in $S_z = 0$ sector and find that it also has the same energy. However, the corresponding state is absent in S_z sectors with $|S_z| > s_G - 1$. Besides, from exact diagonalization of all the states of all the $s_1 - s_2$ alternating spin chains with 8 sites, we find that the energy orderings of the states is such that the lowest excitation is to a state with spin $s = s_G - 1$. We have obtained the excitation gaps for all the three alternating spin chains in the limit of infinite chain length by extrapolating from the plot of spin gap vs. the inverse of the chain length (figure 4). We find that this excitation is gapless in the infinite chain limit for all three cases. This property is quite unusual; the spin systems studied till date with antiferromagnetic exchage interactions have a small correlation length if and only if there is a finite gap to the lowest excited state of the system, from the ground state. Thus, this gapless excitation coexisting with very short correlation length in the ground state can indeed be taken as a signature of systems with spontaneous magnetization.

To characterize the lowest spin excitations completely, we also have computed the energy of the $s = s_G + 1$ state by targetting the lowest state in the $S_z = s_G + 1$ sector. In figure 5, we plot the excitation gaps to the $s = s_G + 1$ state from the ground state for all three systems as a function of the inverse of the chain length. The gap saturates to a finite value of $(1.0221 \pm 0.0001)J$ for the $(\frac{3}{2}, 1)$ case, $(1.8558 \pm 0.0001)J$ for $(\frac{3}{2}, \frac{1}{2})$, and

$(1.2795 \pm 0.0001)J$ for $(1, \frac{1}{2})$. It appears that the gap is also higher when the difference in site spins $|s_1 - s_2|$, is larger. The site spin densities expectation values computed in this state for all three cases are found to be uniform (i.e., independent of the site) on each of the sublattices. This leads us to believe that this excitation cannot be characterized as the states of a magnon confined in a box, as has been observed for a spin-1 chain in the Haldane phase [15].

Earlier studies on pure spin-1 and pure spin-$\frac{1}{2}$ chains [18] have revealed that with the alternation δ in the exchange parameter, the half-odd-integer spin chain will have an unconditional spin-Peierls transition while for integer spin chains, the transition is conditional. This conclusion has been drawn from the fact that, with the inclusion of δ, the magnetic energy gain ΔE can be defined as

$$\Delta E(2N, \delta) \;=\; \frac{1}{2N} \; [\; E(2N, \delta) - E(2N, 0) \;] \;, \tag{7}$$

where $E(2N, \delta)$ is the ground state energy of the $2N$-site system with an alternation δ in the exchange integral, and $E(2N, 0)$ is the ground state energy of the uniform chain of $2N$ sites. For the pure spin chain, if we assume that ΔE varies as δ^ν for small δ, we find that $\nu < 2$ for the half-odd-integer spin chains and $\nu = 2$ for the integer spin chains [18]. Thus, for a half-odd-integer spin chain, the stabilization energy always overcomes the elastic energy, whereas for the integer spin case, it depends on the lattice stiffness.

We have used DMRG calculations extend these studies to the alternating spin systems. We obtain $\Delta E(2N, \delta)$, for small values of δ for all the three alternating spin chains. To determine the exact functional form of the magnetic energy gain, we varied the chain length from 50 sites to 100 sites and also m (the number of states retained in each DMRG iteration) from 80 to 100 to check the convergence of ΔE with chain length. We note that as we approach the classical spin limit, the convergence is reached faster. The dependence of $\Delta E(2N, \delta)$ on $1/2N$ is linear for all three cases for the δ values we have studied. Figure 6 gives a sample variation of $\Delta E(2N, \delta)$ with $1/2N$ for all the systems we have studied. This allows us to extrapolate $\Delta E(2N, \delta)$ to the infinite chain limit reliably for all the cases. In figure 7, we show the plot of $\Delta E(2N, \delta)$ vs. δ for finite $2N$ values and also the extrapolated infinite chain values for all three systems. We see that there is a gain in magnetic energy upon dimerization even in the infinite chain limit for all the systems. To obtain the exponent ν, we plot $\ln \Delta E(2N, \delta)$ vs. $\ln \delta$ for the infinite chain (figure 8). From this figure, we find that in the alternating spin case, for the infinite chain $\Delta E \approx \delta^{2.00 \pm 0.01}$ for all three cases. Thus the spin-Peierls transition appears to be close to being conditional in these systems. The magnetic energy gain per site for finite chains is larger than that of the infinite chain for any value of δ (figure 7). It is possible that the distortion in a *finite* chain is unconditional while that of the infinite chain is conditional for ferrimagnetic systems.

We have also studied the spin excitations in the dimerized alternating (s_1, s_2) chains, defined in equation (1). We calculate the lowest spin excitation to the $s = s_G - 1$ state from

the ground state. We find that the $s = s_G - 1$ state is gapless from the ground state for all values of δ. This result agrees with the spin wave analysis of the general (s_1, s_2) chain. The systems remain gapless even while dimerized unlike the pure antiferromagnetic dimerized spin chains. There is a smooth increase of the spin excitation gap from the ground state to the $s = s_G + 1$ state with increasing δ for all three systems studied here. We have plotted this gap vs. δ in figure 9. The gap shows almost a linear behavior as a function of δ, with an exponent of 1.0 ± 0.01 for all three systems [19]. This seems to be an interesting feature of all ferrimagnets. The spin wave analysis however shows that this excitation gap is independent of δ for the general (s_1, s_2) chain. The similar behaviors of these three alternating spin systems suggest that a ferrimagnet can be considered as a ferromagnet with small quantum fluctuations.

3 Low-Temperature Properties

In this section, we present results of our DMRG calculations of the thermodynamic properties of the $(\frac{3}{2}, 1)$, $(\frac{3}{2}, \frac{1}{2})$ and $(1, \frac{1}{2})$ spin systems. The size of the system varies from 8 to 20 sites. We impose periodic boundary conditions to minimize finite size effects with $\vec{S}_{1,N+1} = \vec{S}_{1,1}$, so that the number of sites equals the number of bonds. We set up the Hamiltonian matrices in the DMRG basis for all allowed S_z sectors for a ring of $2N$ sites. We can diagonalize these matrices completely to obtain all the eigenvalues in each of the S_z sectors. As the number of DMRG basis states increases rapidly with increasing m, we retain a smaller number of dominant density matrix eigenvectors in the DMRG procedure, *i.e.*, $50 \leq m \leq 65$, depending on the S_z sector as well as the size of the system. We have checked the dependence of properties (with m in the range $50 \leq m \leq 65$) for the system sizes we have studied ($8 \leq 2N \leq 20$), and have confirmed that the properties do not vary significantly for the temperatures at which they are computed; this is true for all the three systems. The above extension of the DMRG procedure is found to be accurate by comparing with exact diagonalization results for small systems. It may appear surprising that the DMRG technique which essentially targets a single state, usually the lowest energy state in a chosen sector, should provide accurate thermodynamic properties since these properties are governed by energy level spacings and not the absolute energy of the ground state. However, there are two reasons why the DMRG procedure yields reasonable thermodynamic properties. Firstly, the projection of the low-lying excited state eigenfunctions on the DMRG space in which the ground state is obtained is substantial and hence these excited states are well described in the chosen DMRG space. The second reason is that the low-lying excitations of the full system are often the lowest energy states in different sectors in the DMRG procedure; hence their energies are quite accurate even on an absolute scale.

The canonical partition function Z for the $2N$ site ring can be written as

$$Z \;=\; \sum_j \; e^{-\beta(E_j - B(M)_j)} \;, \tag{8}$$

where the sum is over all the DMRG energy levels of the $2N$ site system in all the S_z sectors. E_j and $(M)_j$ denote the energy and the $\hat{z}$-component of the total spin of the state j, B is the strength of the magnetic field in units of $J/g\mu_B$ (g is the gyromagnetic ratio and μ_B is the Bohr magneton) along the $\hat{z}$ direction, and $\beta = J/k_B T$ with k_B and T being the Boltzmann constant and temperature respectively. The field induced magnetization $< M >$ is defined as

$$< M > \;=\; \frac{\sum_j \; (M)_j \; e^{-\beta(E_j - B(M)_j)}}{Z} \;. \tag{9}$$

The magnetic susceptibility χ is related to the fluctuation in magnetization

$$\chi \;=\; \beta \; [\; < M^2 > - < M >^2 \;] \;. \tag{10}$$

Similarly, the specific heat C is related to the fluctuation in the energy and can be written as

$$C \;=\; \frac{\beta}{T} \; [\; < E^2 > - < E >^2 \;] \;. \tag{11}$$

The dimensionalities of the DMRG Hamiltonian matrices that we completely diagonalize vary from 3000 to 4000, depending upon the DMRG parameter m and the S_z value of the targetted sector, for rings of sizes greater than 12. These matrices are not very sparse, owing to the cyclic boundary condition imposed on the system. The DMRG properties compare very well with exact results for small system sizes amenable to exact diagonalization studies. In the discussion to follow, we present results on the 20-site ring although all calculations have been carried out for system sizes from 8 to 20 sites. This is because the qualitative behavior of the properties we have studied are similar for all the ring sizes in this range for all three systems.

We present the dependence of magnetization on temperature for different magnetic field strengths in figure 10 for all three systems. At low magnetic fields, the magnetization shows a sharp decrease at low temperatures and shows paramagnetic behavior at high temperatures. As the field strength is increased, the magnetization shows a slower decrease with temperature, and for high field strengths the magnetization shows a broad maximum. This behavior can be understood from the type of spin excitations present in these systems. The lowest energy excitation at low magnetic fields is to a state with spin s less than s_G. Therefore, the magnetization initially decreases at low temperatures. As the field strength is increased, the gap to spin states with $s > s_G$ decreases as the Zeeman coupling to these states is stronger than to the states with $s \leq s_G$. The critical field strengths at which the magnetization increases with temperature varies from system to system since this corresponds to the lowest spin gap of the corresponding system. The behavior of the

system at even stronger fields turns out to be remarkable. The magnetization in the ground state ($T = 0$) shows an abrupt increase signalling that the ground state at this field strength has $S_z > s_G$. The temperature dependence of the magnetization shows a broad maximum indicating the presence of states with even higher spin values lying above the ground state in the presence of this strong field. In all three cases, the ground state at very high field strengths should be ferromagnetic. For the systems at such high fields, the magnetization decreases slowly with increase of temperature as no other higher spin states lie above the ground state. While, we have not studied such high field behaviors, we find that the field strength corresponding to switching the spin of the ground state s_G to $s_G + 1$ is higher for $(\frac{3}{2}, \frac{1}{2})$ system compared to $(\frac{3}{2}, 1)$ and $(1, \frac{1}{2})$ systems. The switching field appears to depend on the value of $|s_1 - s_2|$. We see in figure 10 that in the $(\frac{3}{2}, 1)$ and $(1, \frac{1}{2})$ cases, the ground state has switched to the higher spin state at highest magnetic field strength we have studied but in the $(\frac{3}{2}, \frac{1}{2})$ case, the ground state has not switched even at the field strength indicating that the excitation gap for this system is the larger than the other two. For the $(\frac{3}{2}, \frac{1}{2})$ case, the same situation should occur at very high magnetic fields. Thus, we predict that the highest s_z is attained in the ground state at high magnetic field and this field strength increases with increase in site spin difference $|s_1 - s_2|$.

The dependence of magnetization on the magnetic field is shown at different temperatures in figure 11 for all three systems studied here. At low temperature the magnetization shows a plateau. The width of the plateau depends on the system and it decreases as the temperature is raised. Eventually the plateau disappears at higher temperatures. The existence of the plateau shows that the higher spin states are not accessible at the chosen temperature. The plateau is widest in the $(\frac{3}{2}, \frac{1}{2})$ case once again reflecting the larger gap to the $s_G + 1$ state in this system compared with the $(\frac{3}{2} - 1)$ and $(1, \frac{1}{2})$ systems. At higher fields, the larger Zeeman splittings of higher spin states become accessible leading to an increase in the magnetization. The magetization curves at all temperatures intersect at some field strengths depending on the system. For the $(\frac{3}{2}, 1)$ case, the intersection occurs at $B = 1.0J/g\mu_B$ and at higher field strength all the curve collapse. For $(\frac{3}{2}, \frac{1}{2})$ case, the intersection occurs at $B = 1.5J/g\mu_B$, while for the $(1, \frac{1}{2})$ system these curves intersect twice, once at $B = 1.0J/g\mu_B$ and again at $B = 2.5J/g\mu_B$ in the chosen field range. These fields are close to the field strengths at which the ground state switches from one S_z value to a higher value for the corresponding system. Thus, they are strongly dependent upon the actual values of s_1 and s_2.

The dependence of $\chi T/2N$ on temperature for different field strengths are shown in figure 12 for all three systems. For zero field, the zero temperature value of χT is infinite in the thermodynamic limit; for finite rings it is finite and equal to the average of the square of the magnetization in the ground state. For the ferrimagnetic ground state $\chi T/2N$, as $T \to 0$, is given by $s_G(s_G + 1)/6N$. As the temperature increases, this product decreases and shows a minimum before increasing again. For the three systems

studied here, the minimum occurs at different temperatures depending on the system. For the $(\frac{3}{2}, 1)$ alternating spin system, it is at $k_BT = (0.8 \pm 0.1)J$, while for the $(\frac{3}{2}, \frac{1}{2})$ and $(1, \frac{1}{2})$ cases, it occurs at $k_BT = (1.0 \pm 0.1)J$ and $k_BT = (0.5 \pm 0.1)J$ respectively. The minimum occurs due to the states with $S_z < s_G$ getting populated at low temperatures. In the infinite chain limit, these states turn out to be the gapless excitations of the system. The subsequent increase in the product χT is due to the higher energy-higher spin states being accessed with further increase in temperature. This increase is slow in $(\frac{3}{2}, \frac{1}{2})$ case, as in this system very high spin states are not accessible within the chosen temperature range. Experimentally, it has been found in the bimetallic chain compounds that the temperature at which the minimum occurs in the χT product depends upon the magnitude of the spins s_1 and s_2 [13]. The $Ni^{II} - Cu^{II}$ bimetallic chain shows a minimum in $\chi T/2N$ at a temperature corresponding to 55 cm^{-1} $(80K)$; an independent estimate of the exchange constant in this system is 100 cm^{-1} [20]. This is in very good agreement with the minimum theoretically found at temperature $(0.5 \pm 0.1)J$ for the $(1, \frac{1}{2})$ case. The minimum in $\chi T/2N$ vanishes at $B = 0.1J/g\mu_B$ which corresponds to about $10T$ for all three systems. It would be interesting to study the magnetic susceptibility of these systems experimentally under such high fields. The low-temperature zero-field behavior of our systems can be compared with the one-dimensional ferromagnet. In the latter, the spin wave analysis shows that the χT product increases as $1/T$ at low temperatures [21].

In finite but weak fields, the behavior of χT is different. The magnetic field opens up a gap and χT falls exponentially to zero for temperatures less than the gap in the applied field for all three systems. Even in this case a minimum is found at the same temperature as in the zero-field case for the corresponding system, for the same reason as discussed in the zero field case.

In stronger magnetic fields, the behavior of χT from zero temperature upto $k_BT = J_{min}$ (J_{min} is the temperature at which the minimum in χT is observed) is qualitatively different. The minimum in this case vanishes for all three systems. In these field strengths, the states with higher S_z values are accessed even below $k_BT = J_{min}$. The dependence of χT above $k_BT = J_{min}$ at all field strengths is the same in all three systems. In even stronger magnetic fields, the initial sharp increase is suppressed. At very low temperature, the product χT is nearly zero and increases almost linearly with T over the temperature range we have studied. This can be attributed to a switch in the ground state at this field strength. The very high temperature behavior of χT should be independent of field strength and should saturate to the Curie law value corresponding to the mean of magnetic moments due to spin-s_1 and spin-s_2.

The temperature dependence of specific heat also shows a marked dependence on the magnetic field at strong fields. This dependence is shown in figure 13 for various field strengths for all the three systems. In zero and weak magnetic fields, the specific heat shows a broad maximum at different temperatures which are specific to the system. Interestingly, the temperature at which the specific heat shows a maximum closely corresponds

to the temperature where the low-field χT has a minimum for the corresponding system. For a strong magnetic field ($B = J$), there is a dramatic increase in the peak height at about the same temperature corresponding to the specific system, although the qualitative dependence is still the same as at low magnetic fields in all three cases. This phenomena indicates that the higher energy high-spin states are brought to within $k_B T$ of the ground state at this magnetic field strength for all three cases.

Studies of thermodynamic properties of the dimerized alternating spin chains in these three cases show qualitatively similar trends to that of the corresponding uniform systems and follows from the fact that the low-energy spectrum does not change qualitatively upon dimerization.

4 Summary

We have studied alternating spin-$\frac{3}{2}$/spin-1 and spin-$\frac{3}{2}$/spin-$\frac{1}{2}$ systems in detail and compared them with our earlier studies on spin-1/spin-$\frac{1}{2}$ model. The ground state and low-lying excited states have been analyzed by employing the DMRG method and have been compared with the corresponding spin-wave results. The spin of the ground state is given by $s_G = N(s_1 - s_2)$ for a $2N$ site system in all the three cases. There are two types of spin excitations in all the systems. The lowest excitation one is gapless in the infinite chain limit to a state with spin $s_G - 1$. Another excitation to the state with spin $s_G + 1$ is gapped and the gap is larger when the difference in site spins $|s_1 - s_2|$ is an integer. Interestingly, the low-energy spectrum remains qualitatively unchanged upon dimerization, and the dimerization is itself conditional in the infinite chain limit for all the three systems.

We have also employed the DMRG technique to obtain low-temperature thermodynamic properties. For all these cases, the magnetic susceptibility shows very interesting magnetic field dependence. The χT vs. T plot shows a minimum at low-magnetic fields, and the minimum vanishes at high-magnetic fields. The temperature at which this minimum occurs varies from system to system. The specific heat shows a maximum as a function of temperature at all fields. Moreover, the height of the maximum shows a dramatic increase at high-magnetic field. Interestingly, in each system, the temperature corresponding to the maximum in C and minimum in χT is the same at low-magnetic fields.

Acknowledgements

We thank Professor Olivier Kahn who introduced one of us (S.R.) to the experimental alternating spin systems and therby motivated us to undertake this work. The present work has been supported by the Indo-French Centre for the Promotion of Advanced Research through project No. 1308-4, "Chemistry and Physics of Molecule based Materials".

References

[1] Fleming R M, Ramirez A P, Rosseinsky M J, Murphy D W, Haddon R C, Zahurak S M and Makhija A V 1991 *Nature* **352** 787

[2] Allemand P, Khemani K C, Koch A, Wudl F, Holczer K, Donovan S, Gruner G and Thompson J E 1991 *Science* **253** 301

[3] Miller J S, Epstein A J and Reiff W M 1988 *Chem. Rev.* **88** 201

[4] Ovchinnilov A A 1978 *Theor. Chim. Acta* **47** 297

[5] Ramasesha S, Sinha B and Albert I D L 1990 *Phys. Rev.* B **42** 9088; Sinha B and Ramasesha S 1993 *Phys. Rev.* B **48** 16410; Miller J S and Dougherty D A 1989 Proceedings of the Symposium on Ferromagnetic and High-Spin Molecular Based Materials, *Mol. Crys. Liq. Cryst.* **176**

[6] For a review, see Steiner M, Villain J and Windsor C G 1976 *Adv. Phys.* **25** 88

[7] Kahn O 1987 *Structure and Bonding* **68** 89 (Berlin); Kahn 0 1993 *Molecular Magnetism* (VCH: New York)

[8] Kahn O, Pei Y, Verdaguer M, Renard J P and Sletten J 1988 *J. Am. Chem. Soc.* **110** 782; Van Koningsbruggen, Kahn O, Nakatani K, Pei Y, Renard J P, Drillon M and Leggol P 1990 *Inorg. Chem.* **29** 3325

[9] de Vega H J and Woynarovich F 1992 *J. Phys.* A **25** 4499; de Vega H J, Mezincescu L and Nepomechie R I 1994 *Phys. Rev.* B **49** 13223

[10] Alcaraz F C and Malvezzi A L 1996 *Preprint* cond-mat/9611227; Dörfel B -D and Meißner St 1996 *Preprint* hep-th/9609134.

[11] Kolezhuk A K, Mikeska H -J and Yamamoto S 1996 *Preprint* cond-mat/9610097; Brehmer S, Mikeska H -J and Yamamoto S 1996 *Preprint* cond-mat/9610109.

[12] Pati S K, Ramasesha S and Sen D 1997 *Phys. Rev.* B **55** 8894

[13] Kahn O 1995 *Adv. Inorg. Chem.* **43** 179

[14] White S R 1992 *Phys. Rev. Lett.* **69** 2863; 1993 *Phys. Rev.* B **48** 10345

[15] White S R, Huse D A 1993 *Phys. Rev.* B **48**, 3844; Sorenson E S and Affleck I 1994 *Phys. Rev.* B **49** 15771

[16] Hallberg K A, Horsch P and Martinez G 1995 *Phys. Rev.* B **52** R719; Bursill R J, Xiang T and Gehring G A 1994 *J. Phys. A* **28** 2109; Kato Y and Tanaka A 1994 *J. Phys. Soc. Jap.* **63** 1277

[17] Chitra R, Pati S K, Krishnamurthy H R, Sen D and Ramasesha S (1995) *Phys. Rev.* B **52** 6581; Pati S K, Chitra R, Sen D, Krishnamurthy H R and Ramasesha S (1996) *Europhys. Lett.* **33** 707

[18] Schulz H J (1986) *Phys. Rev.* B **34** 6372; Affleck I, Gepner D, Schulz H J and Ziman T 1989 *J. Phys.* A **22** 511; Guo D, Kennedy T and Mazumdar S (1990) *Phys. Rev.* B **41** 9592

[19] Earlier extrapolation in the $(1, \frac{1}{2})$ case was done over the range $\delta \ \epsilon \ 0$ to 0.6. Present extrapolations are for the range $\delta \ \epsilon \ 0$ to 0.1 and hence a small difference from the earlier quoted value of 1.07 in reference [12].

[20] Olivier Kahn, private communication.

[21] Takahashi M (1987) *Phys. Rev.* B **36** 3791

Figure Captions

Figure 1
Extrapolation of the ground state energy per site (ϵ_0), in units of J, as a function of inverse system size.

Figure 2
Expectation values of the z-components of the two spins vs. the unit cell index n. The upper and lower points are for the spin-s_1 and the spin-s_2 sites respectively.

Figure 3
Subtracted two-spin correlation functions as a function of distance between the two spins. (a) spin-s_1 spin-s_1 correlations, (b) spin-s_2 spin-s_2 correlations, and (c) spin-s_1 spin-s_2 correlations. In each figure, squares correspond to $(\frac{3}{2}, 1))$, circles to $(\frac{3}{2}, \frac{1}{2})$ and triangles to $(1, \frac{1}{2})$ systems.

Figure 4
Energy difference (units of J) between the ground state and the lowest energy state with spin $s = s_G - 1$ as a function of inverse system size. s_G is the total spin of the ground state.

Figure 5
Excitation gap (units of J) from the ground state (spin $s = s_G$) to the state with spin $s = s_G + 1$ as a function of the inverse system size.

Figure 6
Gain in magnetic energy $\Delta E(2N, \delta)$ (units of J) associated with dimerization vs. the inverse system size for two different values of dimerization δ. $\delta = 0.025$ (squares) and $\delta = 0.05$ (triangles).

Figure 7
Magnetic energy gain (units of J) as a function of dimerization parameter δ for different system sizes. In the figure $2N = 50$ (squares), $2N = 100$ (circles) and extrapolated values with $N \to \infty$ (triangles) are shown.

Figure 8
Log-log plot of extrapolated magnetic energy gain (units of J) for infinite system size and dimerization parameter δ. Interestingly, the slope is found to be 2.00 ± 0.01 for all the three systems.

Figure 9
Excitation gap (units of J) to the state with spin $s = s_G + 1$ from the ground state ($s = s_G$) as a function of δ for the dimerized alternating chain. The exponent is 1.0 ± 0.01 for all three systems.

Figure 10
Plot of magnetization per site as a function of temperature T for four different values of

the magnetic fields B. Squares are for $B = 0.1J/g\mu_B$, circles for $B = 0.5J/g\mu_B$, triangles for $B = J/g\mu_B$ and diamonds for $B = 2J/g\mu_B$.

Figure 11

Magnetization per site vs. the magnetic field strength B, in units of $J/g\mu_B$, for four different temperatures T. $T = 0.3J/k_B$ results are given by squares, $T = 0.5J/k_B$ by circles, $T = 0.7J/k_B$ by triangles and $T = J/k_B$ by diamonds.

Figure 12

χT (defined in the text) per site as a function of temperature T for various magnetic fields B. Zero field results are shown by squares, $B = 0.01J/g\mu_B$ by circles, $B = 0.1J/g\mu_B$ by triangles and $B = J/g\mu_B$ by diamonds.

Figure 13

Specific heat per site as a function of temperature T for four different values of magnetic fields B. Zero field data are shown by squares, $B = 0.01J/g\mu_B$ by circles, $B = 0.1J/g\mu_B$ by triangles and $B = J/g\mu_B$ by diamonds.

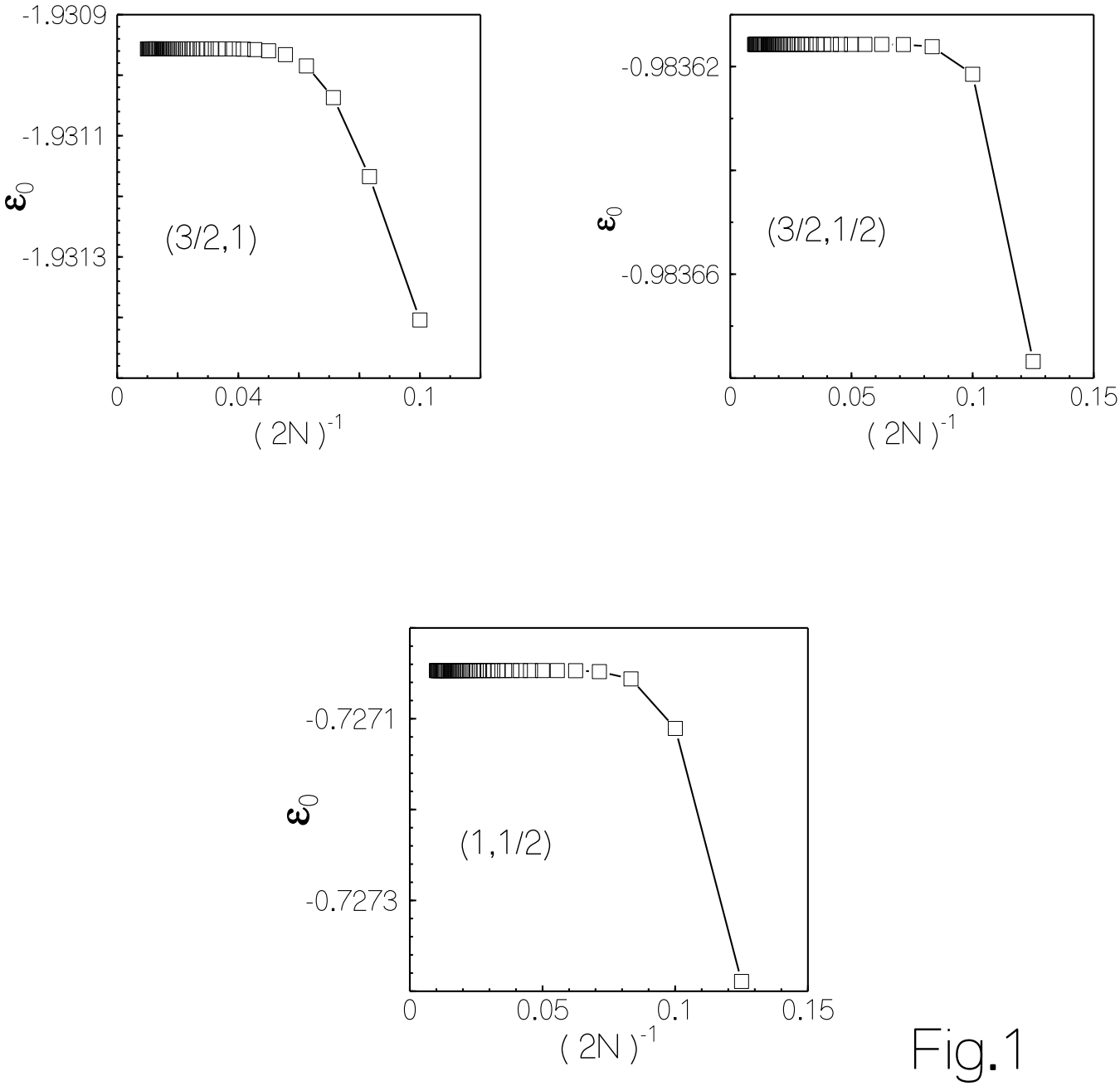
-1.9309
-1.9311
-1.9313
ε_0
(3/2,1)
0
0.04
0.1
$(2N)^{-1}$
-0.98362
-0.98366
ε_0
(3/2,1/2)
0
0.05
0.1
0.15
$(2N)^{-1}$
-0.7271
-0.7273
ε_0
(1,1/2)
0
0.05
0.1
0.15
$(2N)^{-1}$

Fig.1

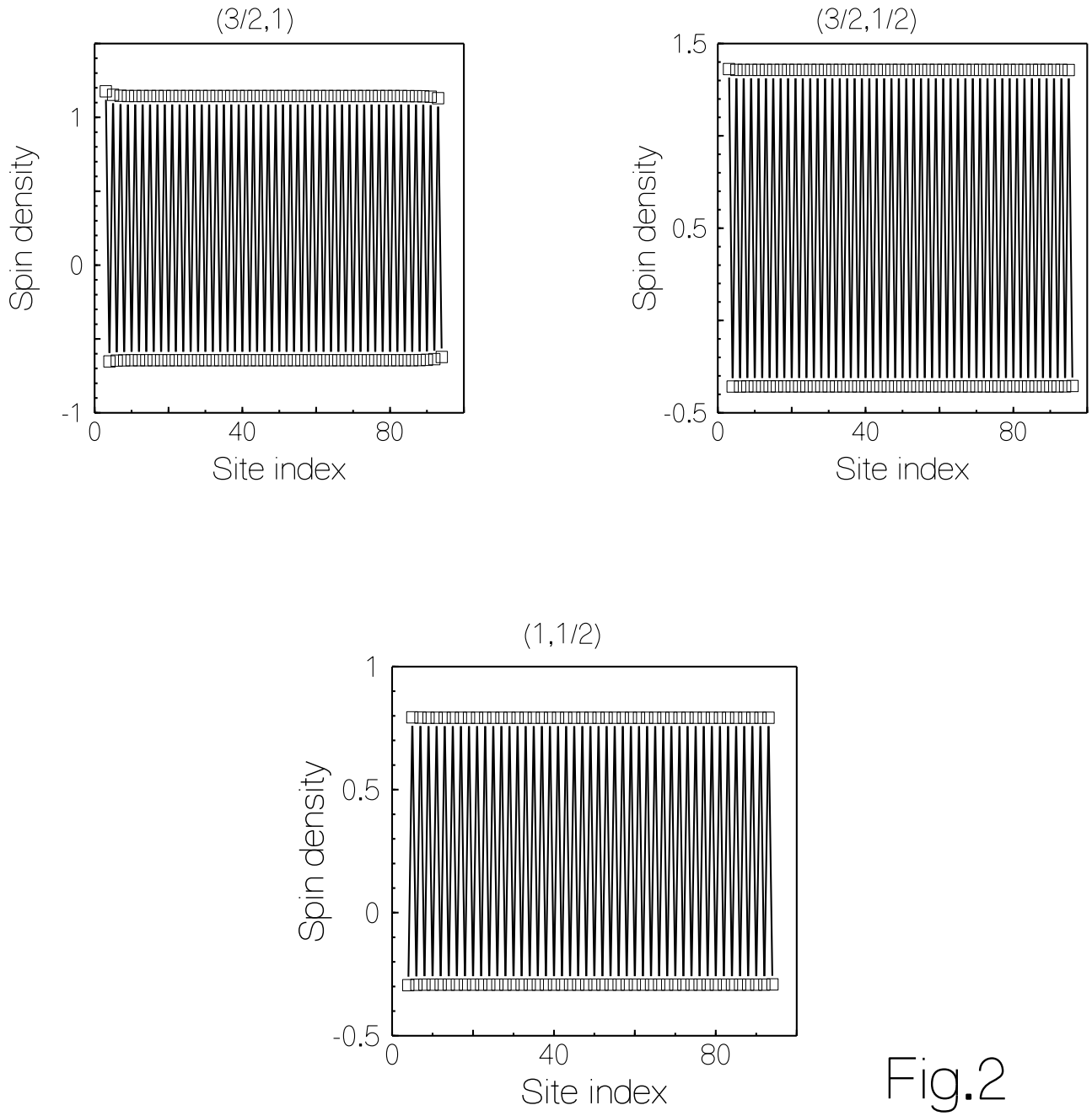
(3/2,1)
Spin density
Site index
1
0
-1
0
40
80
(3/2,1/2)
Spin density
Site index
1.5
0.5
-0.5
0
40
80
(1,1/2)
Spin density
Site index
1
0.5
0
-0.5
0
40
80

Fig.2

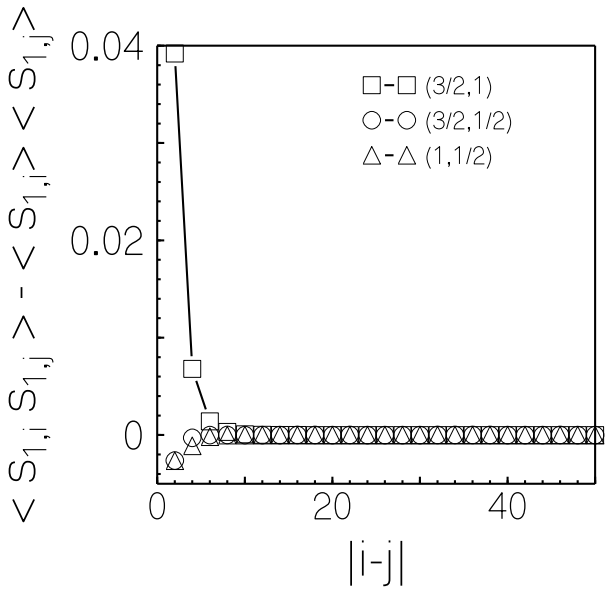
0.04
0.02
0
0
20
40
|i-j|
□-□ (3/2,1)
○-○ (3/2,1/2)
△-△ (1,1/2)
< S1,i S1,j > - < S1,i > < S1,j >

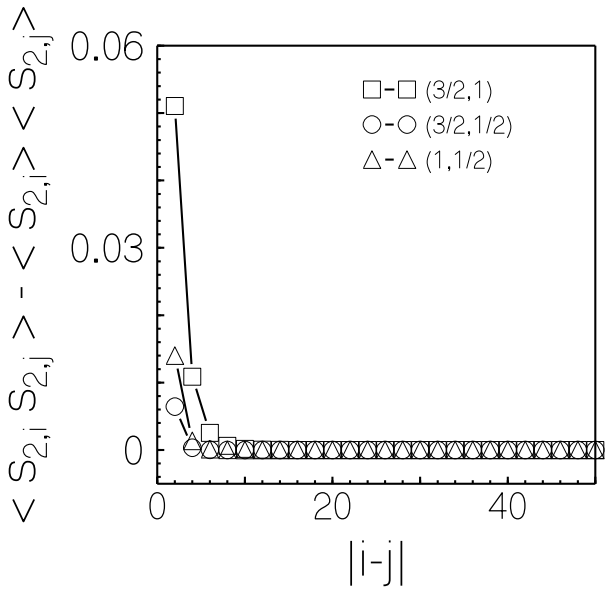
0.06
0.03
0
0
20
40
|i-j|
□-□ (3/2,1)
○-○ (3/2,1/2)
△-△ (1,1/2)
< S2,i S2,j > - < S2,i > < S2,j >

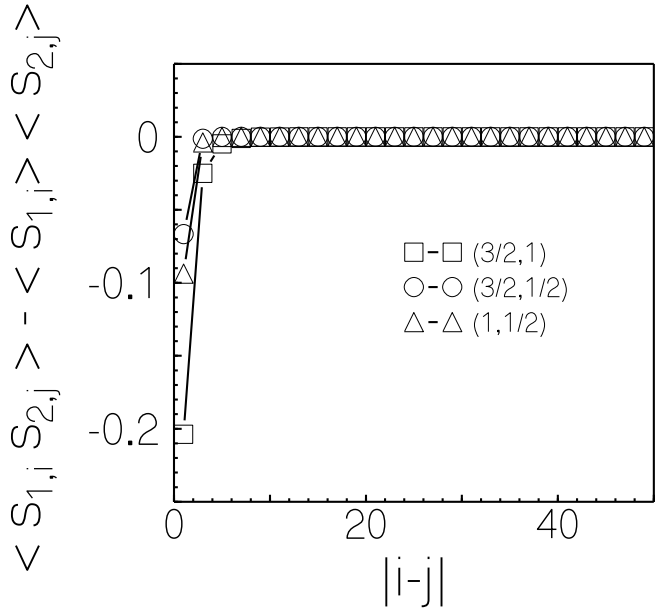
0
-0.1
-0.2
0
20
40
|i-j|
□-□ (3/2,1)
○-○ (3/2,1/2)
△-△ (1,1/2)
< S1,i S2,j > - < S1,i > < S2,j >

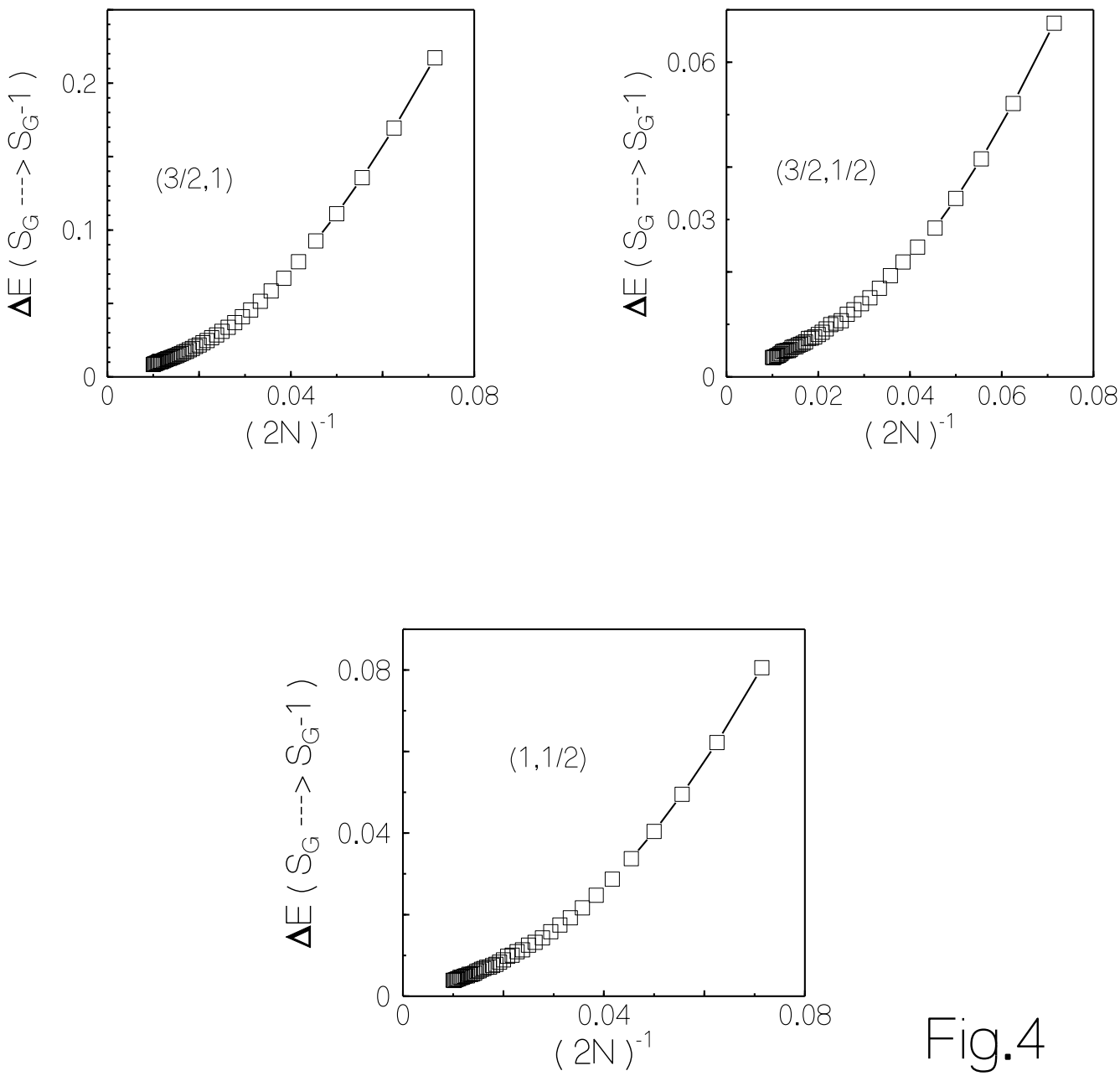

Fig.4

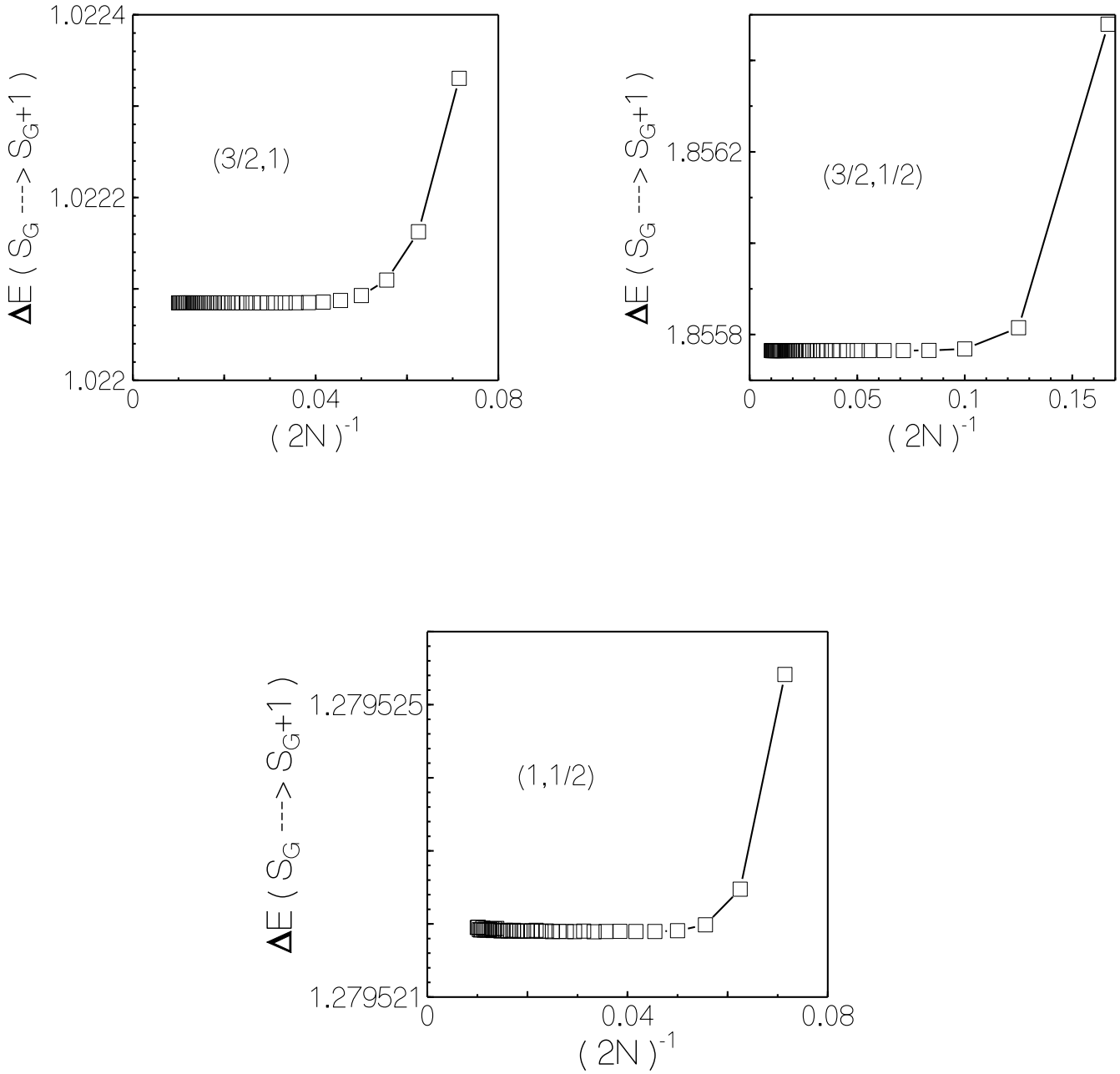
1.0224
1.0222
1.022
0
0.04
0.08
(3/2,1)
ΔE (S_G ---> S_G+1)
(2N)^-1
1.8562
1.8558
0
0.05
0.1
0.15
(3/2,1/2)
ΔE (S_G ---> S_G+1)
(2N)^-1
1.279525
1.279521
0
0.04
0.08
(1,1/2)
ΔE (S_G ---> S_G+1)
(2N)^-1

Fig.5

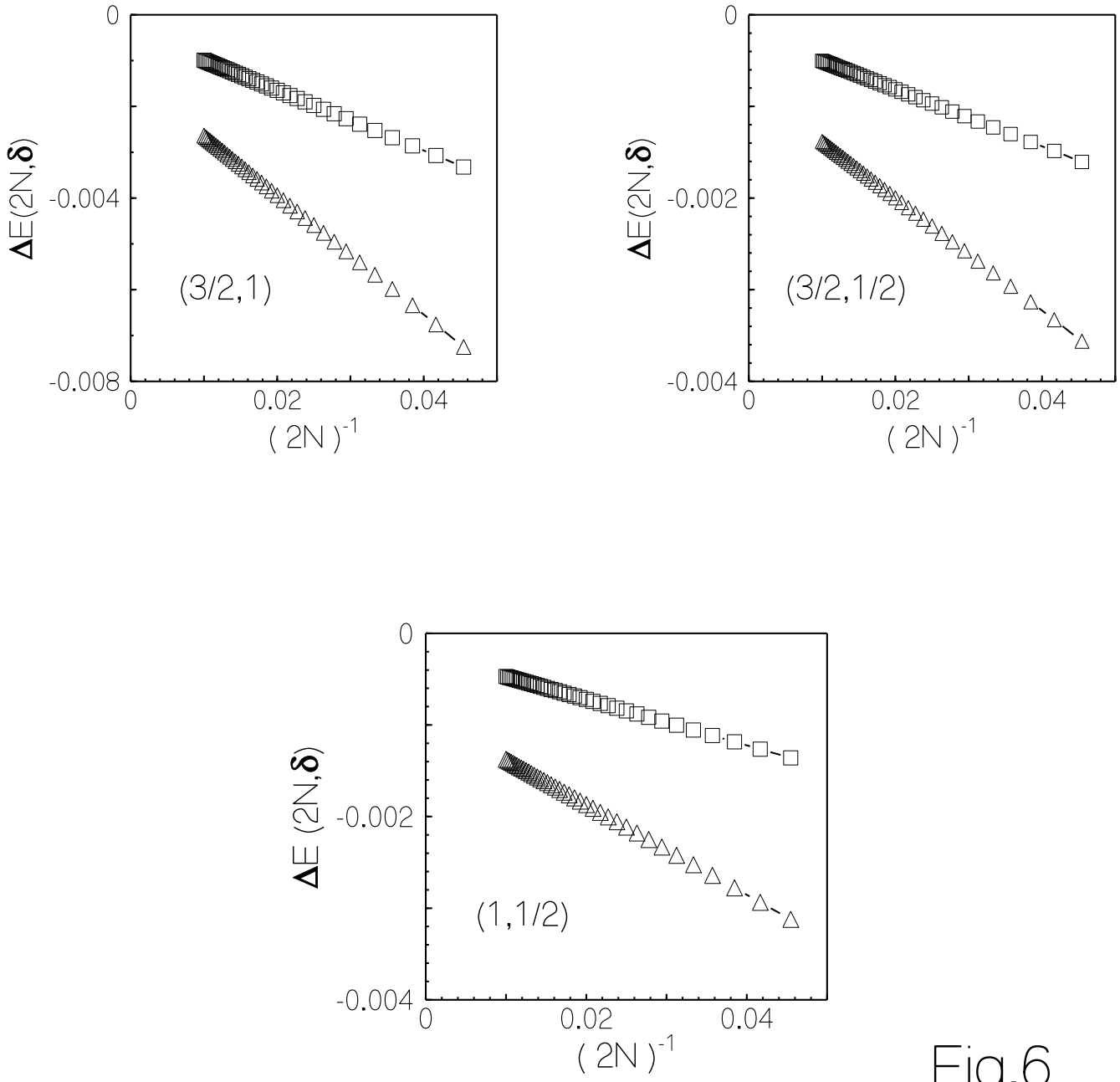
0
-0.004
-0.008
ΔE(2N,δ)
(3/2,1)
0
0.02
0.04
(2N)^-1
0
-0.002
-0.004
ΔE(2N,δ)
(3/2,1/2)
0
0.02
0.04
(2N)^-1
0
-0.002
-0.004
ΔE (2N,δ)
(1,1/2)
0
0.02
0.04
(2N)^-1

Fig.6

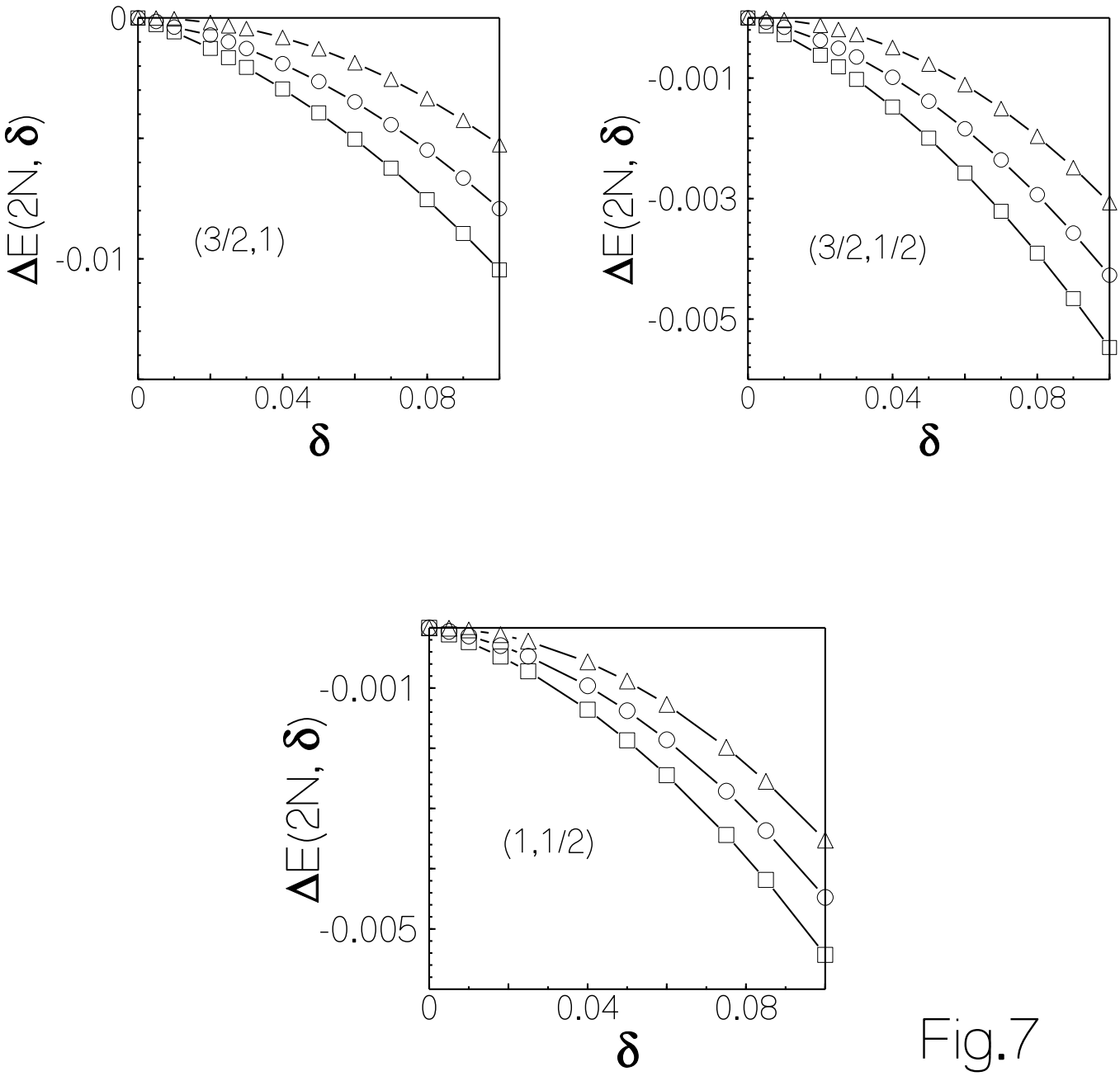
0
-0.01
ΔE(2N, δ)
(3/2,1)
0
0.04
0.08
δ
-0.001
-0.003
-0.005
ΔE(2N, δ)
(3/2,1/2)
0
0.04
0.08
δ
-0.001
-0.005
ΔE(2N, δ)
(1,1/2)
0
0.04
0.08
δ

Fig.7

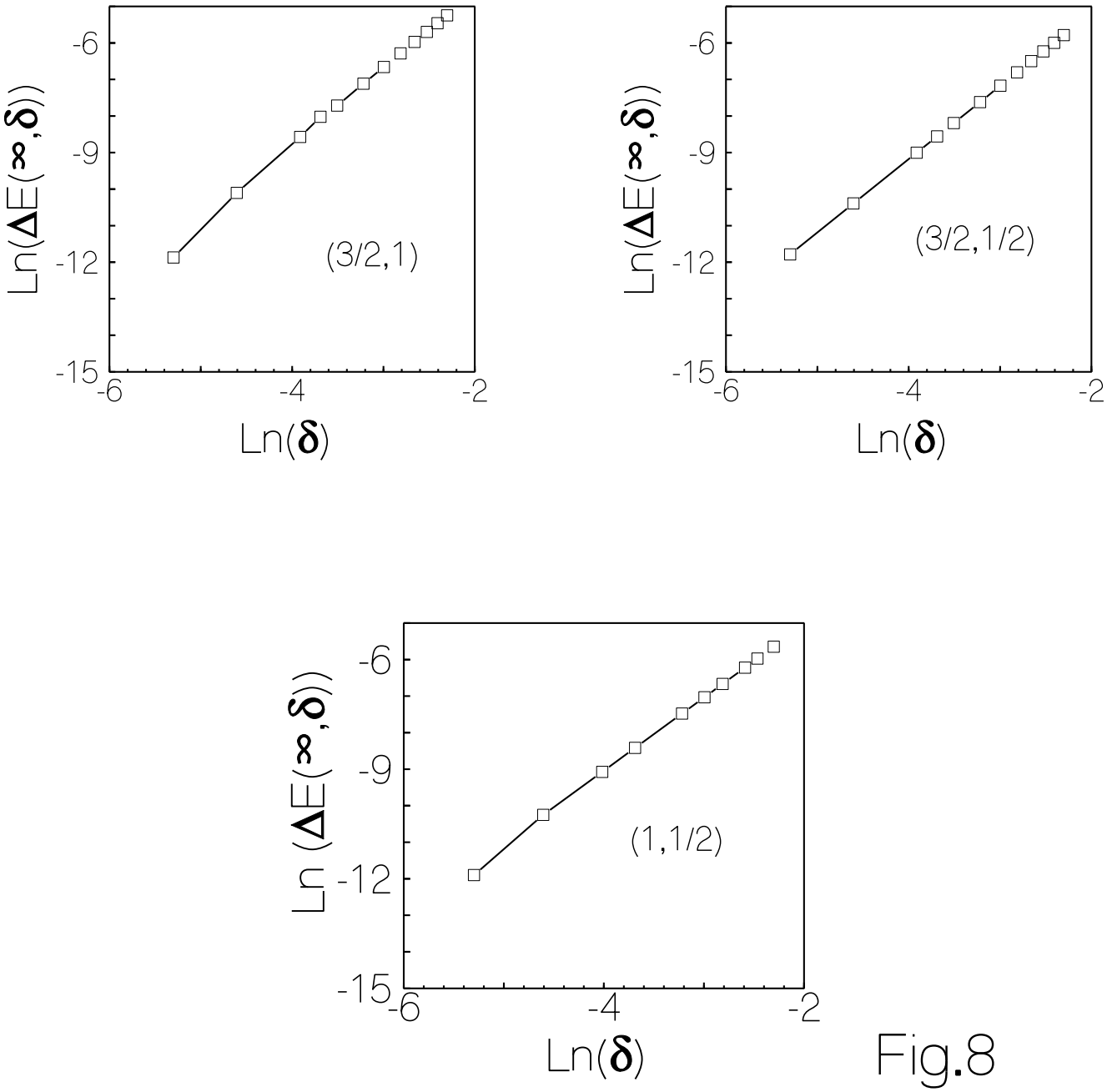

Fig.8

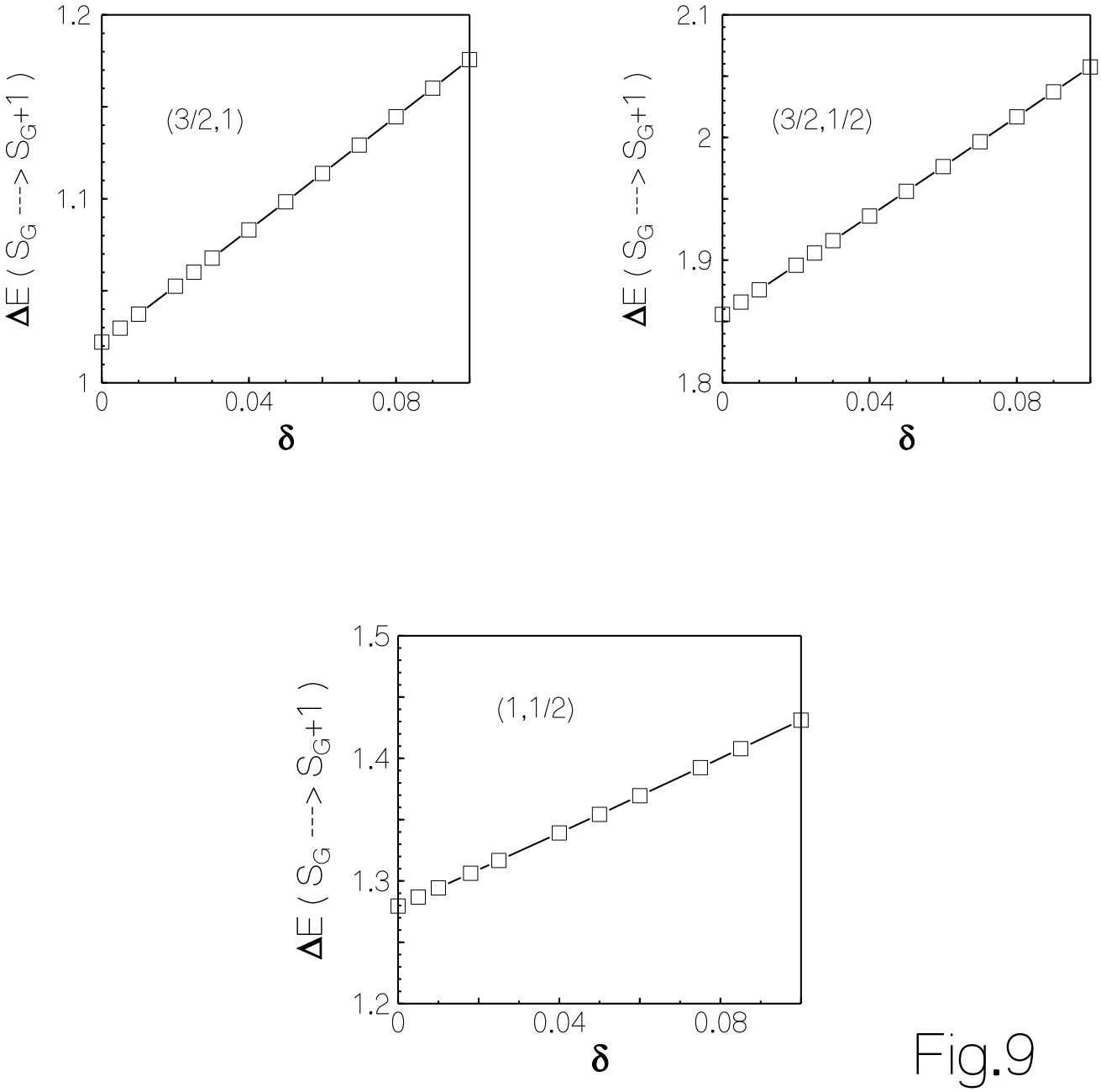

Fig.9

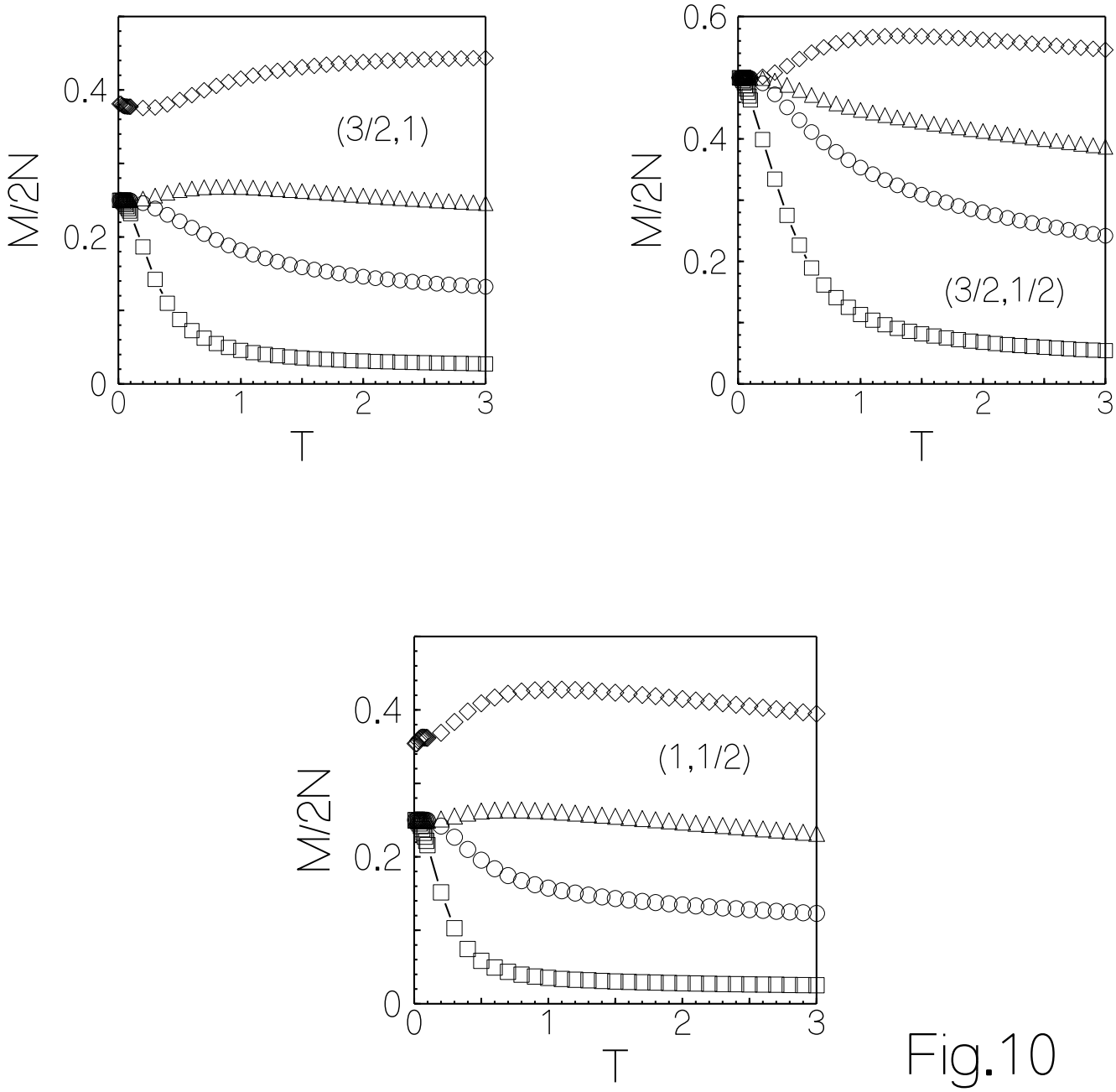

Fig.10

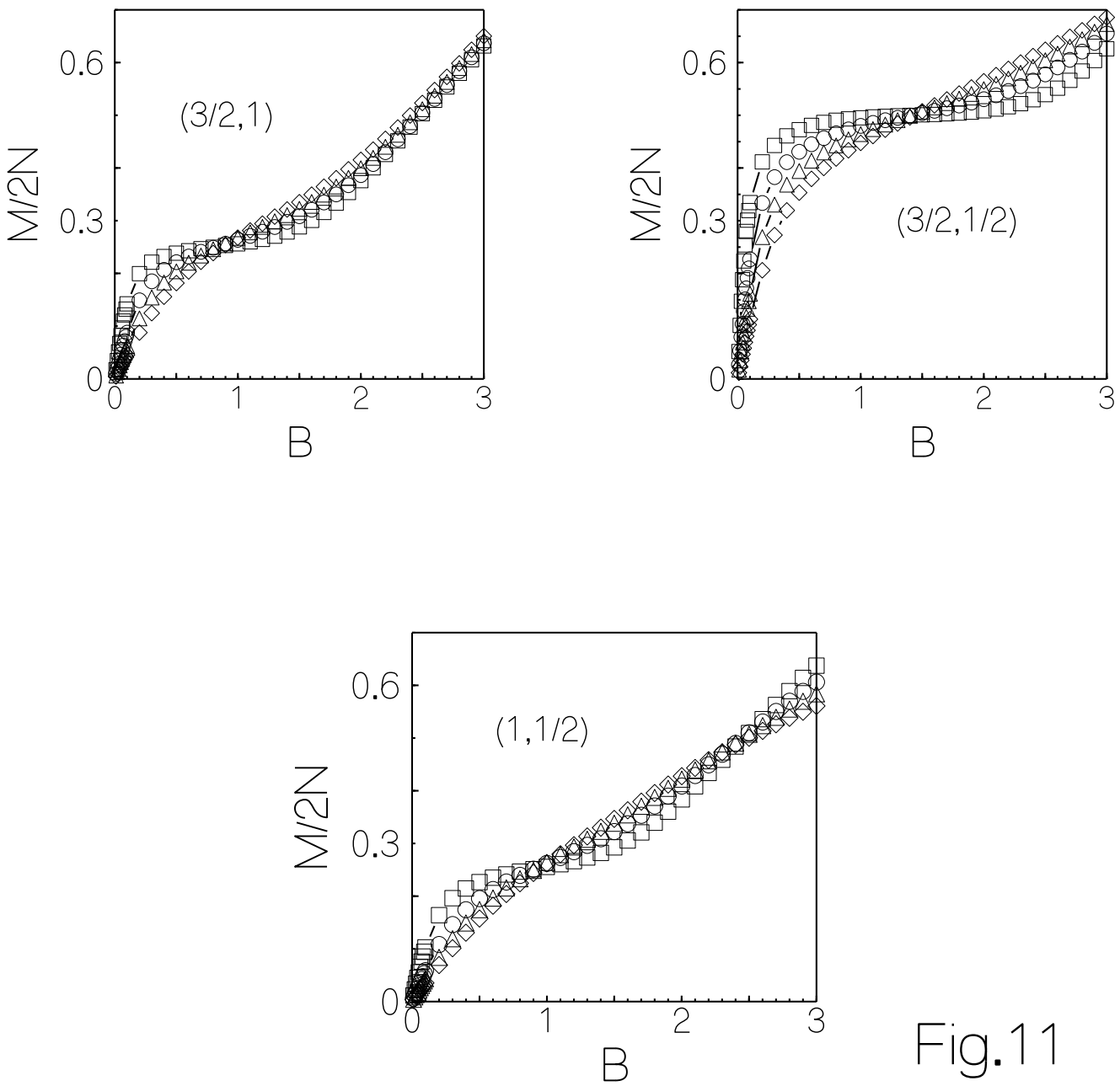

Fig.11

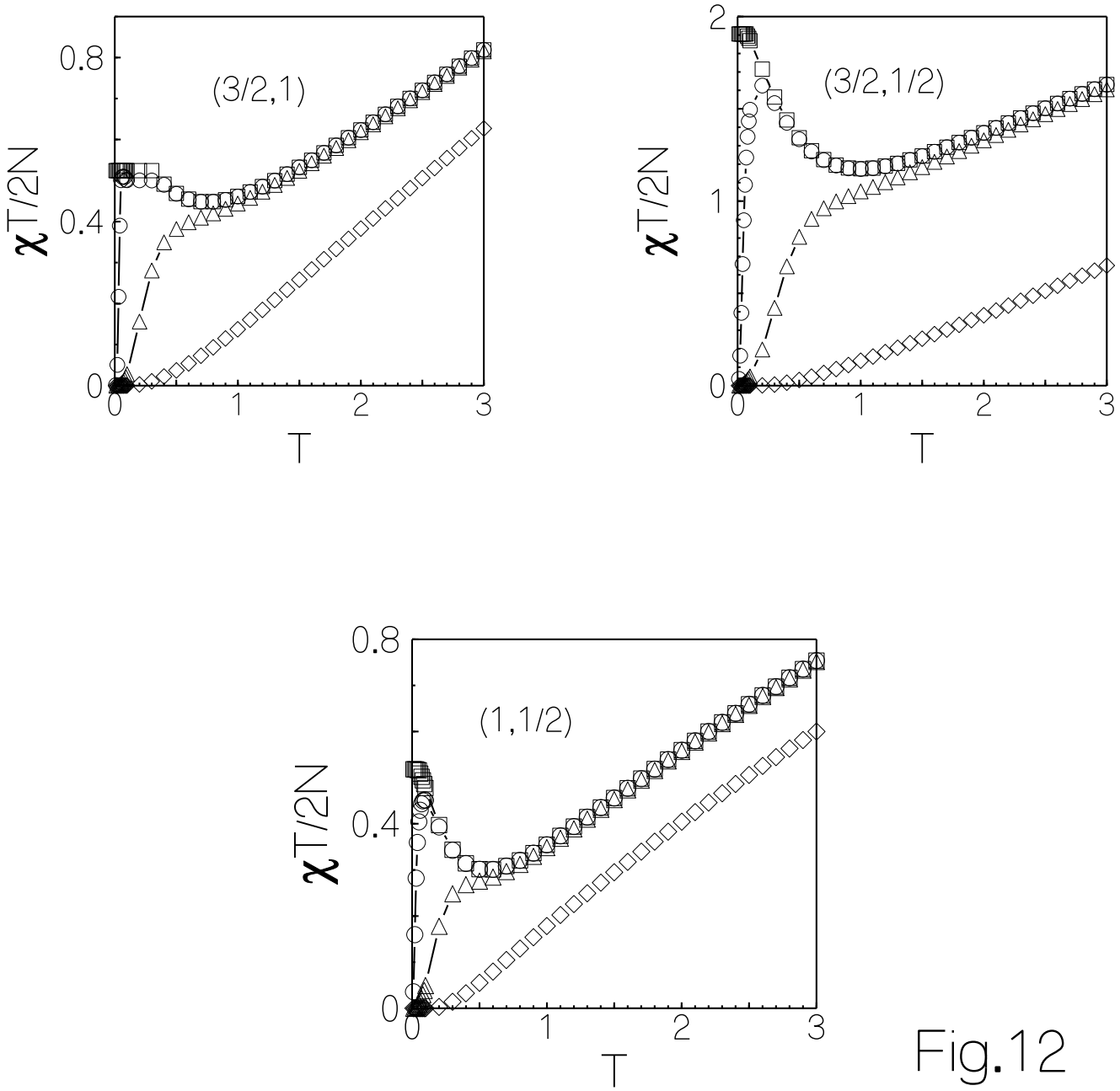

Fig.12

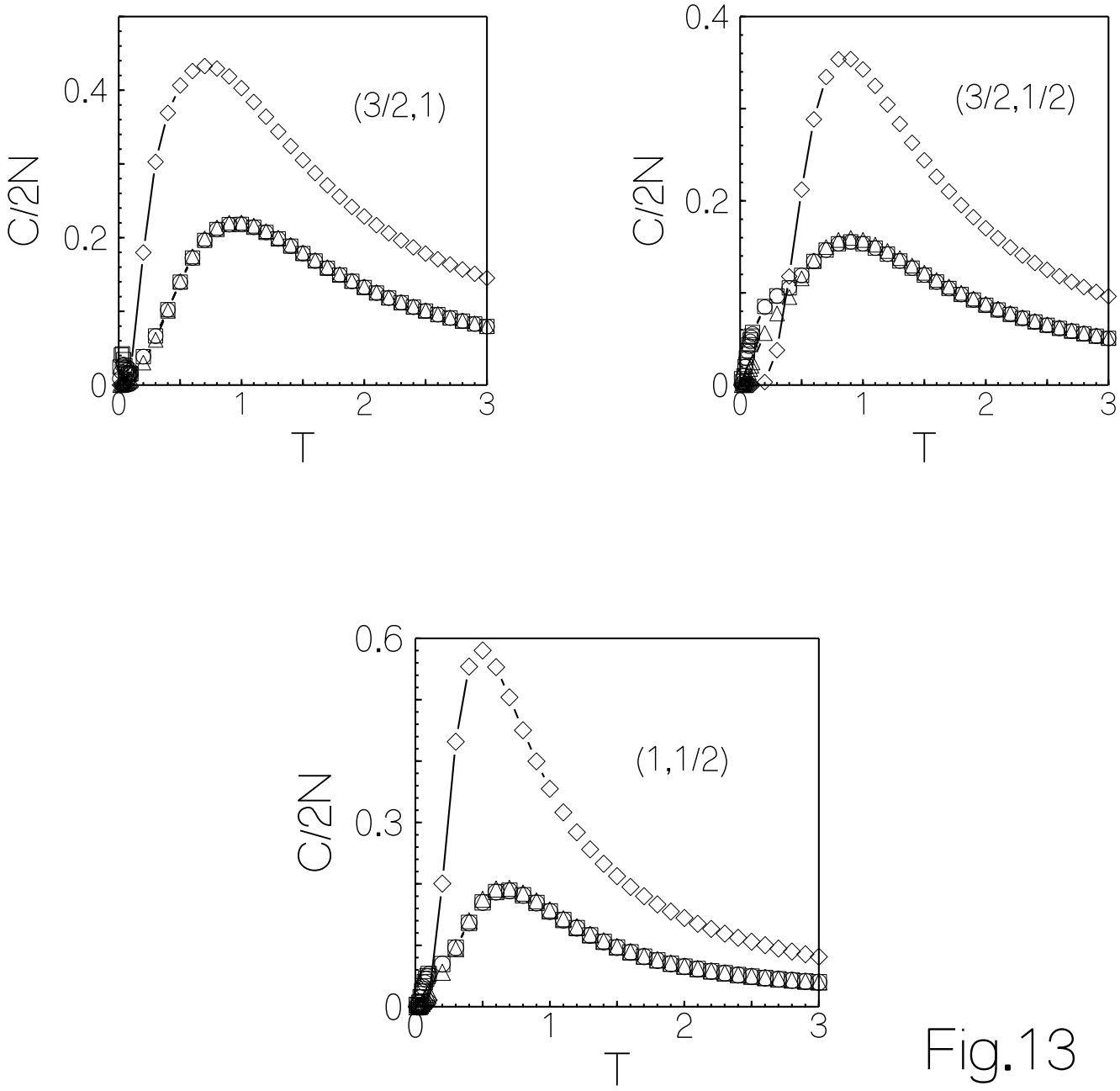

Fig.13